



Open Research Online

Citation

Moore, Elaine (2007). First-principles study of the mixed oxide α -FeCrO₃. Physical Review B, 76(19), article no. 195107.

URL

<https://oro.open.ac.uk/10116/>

License

(CC-BY-NC-ND 4.0) Creative Commons: Attribution-Noncommercial-No Derivative Works 4.0

<https://creativecommons.org/licenses/by-nc-nd/4.0/>

Policy

This document has been downloaded from Open Research Online, The Open University's repository of research publications. This version is being made available in accordance with Open Research Online policies available from [Open Research Online \(ORO\) Policies](#)

Versions

If this document is identified as the Author Accepted Manuscript it is the version after peer review but before type setting, copy editing or publisher branding

Proofs to : Dr E. A. Moore
Department of Chemistry
The Open University
Walton Hall
Milton Keynes
MK7 6AA
United Kingdom

Tel: +441908 655028

Fax: +441908 858327

e-mail: e.a.moore@open.ac.uk

First-principles study of the mixed oxide α -FeCrO₃

Elaine A. Moore

*Department of Chemistry, The Open University, Walton Hall, Milton Keynes MK7
6AA, United Kingdom*

ABSTRACT

We have investigated the electronic and magnetic properties of the mixed oxide α -FeCrO₃ and compared it to the parent oxides α -Fe₂O₃ and α -Cr₂O₃. DFT B3LYP calculations with the non-local Hartree-Fock exchange contribution reduced from 20% to 10% were found to reproduce the band gaps of α -Fe₂O₃ and α -Cr₂O₃ remarkably well. Optimised cell constants also agreed very well with experimental values. Thus this method was used to study α -FeCrO₃. α -FeCrO₃ is predicted to be a charge-transfer insulator with O(2p) and Cr(3d) predominating in the upper edge of the valence band and Fe(3d) in the lower edge of the conduction band. The direct band gap of α -FeCrO₃ is predicted to be close in value to that of α -Fe₂O₃. For ordered α -FeCrO₃ the lowest energy is found for chromium ions occupying the sites related by the c glide plane. The antiferromagnetic ground state of this oxide is found to be that with magnetic ordering as in α -Fe₂O₃.

I. INTRODUCTION

α -Fe₂O₃ and α -Cr₂O₃ both adopt a corundum-like structure, but display differences in the magnetic ordering of the cations and in the nature of the bands either side of the Fermi level. In the primitive rhombohedral unit cell of the non-magnetic or ferromagnetic corundum structure, there are four symmetry-related metal ions aligned on the 3-fold axis with z-coordinates 0.15, 0.35, 0.65 and 0.85, Figure 1. Following Catti et al¹, we label these 1, 2, 3 and 4 in order of increasing z coordinate, as indicated on the figure. The pairs 1, 2 and 3, 4 are related by 2-fold axes at $z = 0.25$ and $z = 0.75$; the pairs 2, 3 and 4, 1 are related by symmetry centres at $z = 0$ and $z = 0.5$ and the pairs 1, 3 and 2, 4 are related by the c glide plane. The ferromagnetic state retains the full $R\bar{3}c$ symmetry. For the antiferromagnetic state there are three possibilities of lower symmetry – $R3c(\uparrow\downarrow\uparrow\downarrow)$, $R\bar{3}(\uparrow\downarrow\uparrow)$ and $R32(\uparrow\uparrow\downarrow\downarrow)$ where the arrows represent the relative orientation of spins on positions 1, 2, 3 and 4 in that

order. Neutron diffraction experiments^{2,3} have shown that below the Néel temperature, α -Cr₂O₃ adopts the R3c structure and α -Fe₂O₃ the $R\bar{3}$ structure. Thus for both oxides spin coupling is antiferromagnetic between the pairs of cations with the longer separation (1, 2 and 3, 4), but is ferromagnetic for pairs separated by the shorter distance (2, 3 and 4, 1) in α -Fe₂O₃ and antiferromagnetic in α -Cr₂O₃. Spectroscopic evidence⁴ suggests that α -Fe₂O₃ is a charge-transfer insulator with a band gap between a lower predominantly O2p band and an upper Fe3d band. By contrast photoemission studies⁵ and inverse photoemission experiments⁶ support classification of α -Cr₂O₃ as an intermediate-type insulator between charge-transfer and Mott-Hubbard insulator.

The mixed oxides α -Fe_{2-x}Cr_xO₃ also adopt the corundum structure forming a solid solution retaining this structure throughout the range 100% α -Cr₂O₃ to 100% α -Fe₂O₃ with a smooth increase in unit cell volume⁷ but a very strong deviation from Vegard behaviour suggesting either cation ordering or specific magnetic interactions between cations. The solid solutions are antiferromagnetic with a single Néel temperature that decreases linearly with increasing proportion of Cr. There is no evidence of superstructure peaks in the diffraction pattern⁸ suggesting that Fe and Cr occupy the cation sites in a random manner, although an earlier study of the vibrational spectrum⁹ suggested that α -FeCrO₃ adopted an ilmenite-like $R\bar{3}$ structure. For x = 0.8, 1.0 and 1.2 powder neutron diffraction lines are consistent with the spin ordering of α -Fe₂O₃⁸. There are however changes in the magnetic ordering below the Neel temperature for x = 1.6⁸.

These oxides pose a challenge to computation because the metal d electrons are strongly correlated. There have been a number of computational studies of the pure transition metal sesquioxides using both unrestricted Hartree-Fock (UHF) and density

functional theory (DFT) methods. Catti et al¹⁰ used the unrestricted Hartree-Fock (UHF) method within the linear combination of crystalline orbitals (LCCO) approach. This grossly overestimated the size of the band gap but correctly predicted that Fe₂O₃ was a charge transfer insulator and Cr₂O₃ a borderline charge transfer/Mott-Hubbard insulator. The overestimation of the band gap is due to complete neglect of correlation. A DFT study¹¹ using the augmented spherical wave (ASW) method with a local spin density approximation (LSDA) functional underestimated the band gap but, when the results were adjusted for this, produced a good fit to the spectroscopic data. Using an LSDA functional with a tight-binding approach¹², Punkkinen et al obtained a value of 1.42 eV for the energy band gap by including a Hubbard-type on-site Coulomb repulsion in the Hamiltonian (LSDA + U method). It should be noted however that these two latter studies fixed the cell parameters at the experimental values. Bandyopadhyay et al¹³ found that using LSDA and LSDA + U within a plane wave code using projector augmented wave (PAW)-based pseudopotentials and relaxing the structure yielded values of 0.31 eV and 1.88 eV respectively for the band gap. A standard pseudopotential plane-wave study of α -Cr₂O₃¹⁴ reproduced the structural properties well but the band gap was underestimated at ~1.5 eV. Using a generalised gradient approximation (GGA) density functional¹⁵ gives band gaps that are too small for both α -Fe₂O₃ and α -Cr₂O₃. However including strong correlation effects described by a Hubbard-type on-site Coulomb repulsion (GGA + U) leads to very good agreement with the size of the band gap and the nature of the orbitals contributing to the bands¹⁵, although the predicted band gaps of the two solids are closer to each other than found experimentally. Using the hybrid DFT functional B3LYP within the LCCO approach has been shown to predict correctly the ground states of strongly correlated electronic systems and the band gap, including that of

α -Cr₂O₃¹⁶. B3LYP corresponds to Becke's GGA exchange functional¹⁷ with the correlation potential of Lee, Yang and Parr¹⁸ and with 20% of the exchange functional replaced by the exact Hartree-Fock exchange.

One of our aims is to investigate how well the B3LYP functional describes α -Fe₂O₃ and α -Cr₂O₃ in terms of band gap, nature of the valence and conduction bands and magnetic ordering. Given the differing magnetic ordering and nature of the bands either side of the band gap, particularly the valence band, in these two oxides, we were also interested in investigating the properties of the mixed oxide α -FeCrO₃. We have chosen to study ordered structures of the mixed oxide with the same number of ions in the unit cell as the pure oxides. This enabled us to consider antiferromagnetic solutions without recourse to supercells. The chosen structures are sufficient to determine whether coupling between Fe and Cr ions will be ferromagnetic or antiferromagnetic for both the long and short separations of the ions and thus is relevant to spin-ordering in both random and ordered α -Fe_{2-x}Cr_xO₃. In addition, although α -Fe_{2-x}Cr_xO₃ produced via a high temperature route may well have a random ordering of Fe and Cr over the cation sites, it is possible that the most energetically favoured state at low temperatures, where calculations of this kind are valid, would be ordered. A study¹⁹ of Cr-doped α -Fe₂O₃ using LSDA + U with one Cr substituting for Fe in a 30-atom unit cell, suggested that the filled Cr impurity level lay close to the top of the valence band and that consequently the band gap was unchanged from that of α -Fe₂O₃. We were interested to see if this would remain the case for 50% substitution on the Fe sites.

II. COMPUTATIONAL METHODS

Electronic and magnetic properties and the band structure of the oxides were calculated using CRYSTAL03²⁰ and CRYSTAL06²¹ on the Linux beowulf cluster at The Open University and on the Linux Opteron beowulf cluster (formerly COMPAQ 8400), Columbus, at The Rutherford Appleton Laboratory. The basis sets used for Fe, Cr and O were taken from the literature¹⁰. The tolerances used as the truncation criteria for bielectronic integrals were 10^{-7} , 10^{-7} , 10^{-7} , 10^{-7} and 10^{-14} . Calculations were performed on the ferromagnetic state and the possible antiferromagnetic states. For α -FeCrO₃ all arrangements of the metal ions within the unit cell were studied. Cell constants and atomic positions were both optimised for α -Fe₂O₃, α -Cr₂O₃ and α -FeCrO₃ using the DFT method with the hybrid functional B3LYP in CRYSTAL06. A recent study²² showed that using B3LYP with the non-local Hartree-Fock exchange contribution increased from 20% to 35% gave very accurate values for spin-spin coupling constants in a series of transition metal compounds. However it was subsequently suggested that the optimum exchange contribution differed for direct exchange and superexchange²³ and that for the solids studied, 35% was a compromise between the two.

We therefore investigated the effect of changing the percentage of the non-local Hartree-Fock exchange contribution. A series of runs on α -Fe₂O₃ with the experimental cell parameters and varying Hartree-Fock exchange contributions was performed. Values of the energy band gap decreased roughly linearly with decreasing percentage of Hartree-Fock exchange contribution with a discontinuity between 25% and 22%. This coincided with a change from pure O2p character of the top levels of the valence band to a mixed Fe3d /O2p character. A Hartree-Fock exchange contribution of 10% gave a band gap close to the experimental one. Consequently we

performed runs on α -Fe₂O₃, α -Cr₂O₃ and α -FeCrO₃ with optimisation of both cell constants and atomic positions using a 10% Hartree-Fock exchange correlation.

III. RESULTS AND DISCUSSION

A. Crystal structure

The calculated energies of the ferromagnetic and the possible antiferromagnetic states for FeCrO₃ with the different possible arrangements of Fe and Cr on the cation sites are given in Table I.

The lowest energy state of α -FeCrO₃ is found to be that with the cations arranged FeCrFeCr in ascending order of *z* coordinate along the three-fold axis. We have also obtained this arrangement of cations as the lowest energy arrangement using interatomic potential calculations. The determining factor in the distribution of Fe and Cr ions is thus likely to be steric rather than electronic. We note that our calculations show that the centrosymmetric arrangement is not the most stable ordered form as an early experimental report suggested⁹.

Optimisation of both the cell constants and atomic positions for the lowest energy antiferromagnetic state using DFT with the hybrid B3LYP functional gave values very close to experimental values. We also performed such optimisations for both α -Fe₂O₃ and α -Cr₂O₃ for comparison and the results are given in Table II. Our results show considerable improvement over the published UHF optimised structure and are comparable to the results of Hafner et al using the plane wave GGA method with the addition of Hubbard-type on-site Coulomb repulsion¹⁵. We note that our values for *a* and *c* show a marked decrease from α -Fe₂O₃ to α -Cr₂O₃ in agreement with experiment and in contrast to the GGA + U results which give very similar structures for these two oxides. Calculations using B3LYP with the Hartree-Fock exchange

contribution decreased from 20% to 10% which gave the most accurate band gaps (see below) gave slightly less good agreement with the experimental structure, although there was still a marked decrease in the parameters for α -Fe₂O₃ and α -Cr₂O₃ in line with experiment. Even for these calculations, the largest error (in the c axis of α -Fe₂O₃ and α -Cr₂O₃) was only 1.4% which is extremely good agreement for calculated lattice parameters.

The cation arrangements FeCrFeCr and FeFeCrCr gave very similar lattice parameters for the lowest energy antiferromagnetic state. For FeCrCrFe, the cell constants were slightly larger. All three results are however sufficiently close that a mixture of all three in the crystal would be feasible without causing substantial strain.

B Magnetic Properties

In the non-magnetic or ferromagnetic corundum structure, the primitive rhombohedral unit cell contains four symmetry-related cations aligned along the threefold axis which, following Catti et al¹, we labelled 1, 2, 3, 4 with increasing z coordinate in Figure 1. The stable antiferromagnetic state for α -Fe₂O₃ is characterised by the spin sequence $\uparrow\downarrow\downarrow\uparrow$ and that for α -Cr₂O₃ by the spin sequence $\uparrow\downarrow\uparrow\downarrow$. In both cases the spin sequence $\uparrow\uparrow\downarrow\downarrow$ is the next most stable antiferromagnetic state.

In Table I we presented results for all arrangements of both Fe and Cr ions and all possible spin states. The positions of Fe and Cr ions in the structure are given in the order 1, 2, 3, 4. The blank entries refer to spin states in which both Cr ions have the same spin which is opposed to that on both Fe ions. In these cases, since the Fe and Cr ions have different numbers of unpaired electrons, the solids will be ferrimagnetic rather than antiferromagnetic. From Table I we predicted that the lowest energy antiferromagnetic state of α -FeCrO₃ is one with Fe on sites 1 and 3 and Cr on sites 2

and 4. The lowest energy magnetic ordering for this arrangement of cations is the same as for pure hematite, $\uparrow\downarrow\uparrow$. We also considered the spin states of other orderings of Fe and Cr on the cation sites. For the cation order FeFeCrCr the lowest energy spin arrangement is again $\uparrow\downarrow\uparrow$ as for FeCrFeCr. However for the order FeCrCrFe, this arrangement would not be antiferromagnetic. The lowest antiferromagnetic state for this arrangement is $\uparrow\downarrow\downarrow$. The energy difference between this state and the higher energy antiferromagnetic state is much smaller than the comparable energy difference for the other two cation orders.

For the lowest energy states for all three orders of cations, coupling between the cations separated by the longer distance is antiferromagnetic. This is not unexpected as both FeFe coupling and CrCr coupling are antiferromagnetic across this distance.

From the results for the arrangements FeFeCrCr and FeCrFeCr we conclude that coupling between Fe and Cr ions separated by the shorter distance is ferromagnetic.

For FeCrCrFe we would thus expect cations on sites 1 and 2 and on sites 3 and 4 to be antiferromagnetically coupled, the Cr ions on sites 2 and 3 to be antiferromagnetically coupled and the Fe ions on sites 4 and 1 to be ferromagnetically coupled. It is impossible for all these couplings to be satisfied. Thus this is a potentially spin-frustrated situation and may give rise to a spin glass.

The difference in the signs of the various spin-couplings in these oxides can be rationalised by considering the nature of the superexchange in these oxides. It has previously been noted¹ that superexchange in corundum-type structures is not simply a function of cation-cation distance. In the corundum-type structure, the M-O-M' angle is less than the ideal σ -type superexchange value of 180° and is smaller for the cations separated by the shorter distance. However π -type superexchange, whilst weaker than σ -type superexchange at 180° , is still effective at an M-O-M' angle of

90°. In α -Fe₂O₃, the 3d orbitals that contribute to π -type superexchange are low in energy and do not interact well with O2p orbitals. Consequently superexchange in Fe₂O₃ is dominated by σ -type interactions. The Fe-O-Fe angle for the shorter Fe-Fe distance is close to 90° where such interaction is ineffective and the spin-spin interaction is dominated by direct exchange giving ferromagnetic coupling. In α -Cr₂O₃ by contrast, superexchange is π -type and the cations separated by the shorter distance are antiferromagnetically coupled via superexchange. From our results it would appear that Fe-O-Cr interactions are dominated by σ -type superexchange. This is not unexpected as π -type superexchange would still be inhibited by the lack of strong interaction between the relevant Fe3d orbitals and O2p orbitals. Calculated magnetic moments tend to be close to experimental for UHF calculations but low for DFT calculations and this is true here. The calculated magnetic moments are included in Table II.

C. Band structure

UHF calculations are known to give band gaps that are far too large, but calculations on α -Fe₂O₃ and α -Cr₂O₃¹⁰ predict the correctly the nature of the orbitals either side of the band gap. DFT calculations generally give band gaps that are too small but recent calculations^{13, 15} involving addition of a Hubbard-type on-site Coulomb interaction give band gaps close to experiment for these oxides.

Our DFT B3LYP calculations give band gaps that are reasonably close to experiment but are too large. In the light of the success of the +U method calculations, we decided to try the effect of varying the percentage of non-local Hartree-Fock exchange contribution. Following our exploration of the effect of varying the percentage on the band gap of α -Fe₂O₃ (see computational method), we tried fully optimised calculations with a non-local Hartree-Fock exchange contribution of 10% and found

this gave a band gap close to experiment for both α -Fe₂O₃ and α -Cr₂O₃. The results of our calculations with both standard DFT B3LYP and with the non-local Hartree-Fock exchange contribution changed to 10% are given in Table II. The band gap for α -FeCrO₃ is predicted to be close to that of α -Fe₂O₃ for both standard B3LYP and for B3LYP with the non-local Hartree-Fock exchange contribution changed to 10%, for all distributions of Fe and Cr over the cation sites.

Figure 2 compares the total density of states and the projections of metal 3d and O2p on to the density of states for the pure oxides. This figure shows clearly that the bottom of the conduction band is dominated by metal 3d orbital contributions.

However whereas in α -Fe₂O₃ two narrow Fe3d-dominated bands arise, in α -Cr₂O₃ the empty Cr3d-dominated band is much broader. The valence band of α -Cr₂O₃ is dominated by Cr3d orbitals with some admixture of O2p orbitals in line with the experimental description of this oxide being an intermediate-type insulator between charge-transfer and Mott-Hubbard insulator. By contrast the valence band of α -Fe₂O₃ contains both Fe3d and O2p orbitals with a predominance of O2p at the band edge. The Fe3d orbitals at the top edge of the valence band come from a different set of atoms (on sites 2 and 3) to those (on sites 1 and 4) contributing to the lower edge of the conduction band. Thus we would predict this oxide to be a charge-transfer insulator as is found experimentally. The appearance and nature of the α -Fe₂O₃ bands are very similar to those obtained by several authors^{12, 13, 15} using GGA + U or LSDA + U methods.

The total density of states and projections of metal 3d and O2p onto the density of states are shown for all the lowest energy antiferromagnetic states of ordered α -FeCrO₃ in Figure 3. These are very similar. The lower edge of the conduction band is dominated by two narrow Fe3d bands as for α -Fe₂O₃. Cr 3d bands lie above this. In

α -FeCrO₃ there are two distinct Cr3d bands as opposed to the continuous broad band found for α -Cr₂O₃. The top of the valence band is dominated by Cr3d but this overlaps the O2p-dominated mixed Fe/O bands. The upper edge of this band thus remains at roughly the same energy as in the pure oxides and because the direct band gap is taken as the difference between the bottom of the conduction band and the top of the valence band, the predicted band gap is very similar to that of α -Fe₂O₃. This band structure resembles that of Cr-doped hematite¹⁹. We consider the most likely lowest energy transition across the band gap to be from O2p to Fe3d and therefore classify α -FeCrO₃ as a charge transfer insulator.

IV CONCLUSIONS

Ab initio LCCO DFT B3LYP calculations with the non-local Hartree-Fock exchange contribution decreased to 10% gave values close to experiment for the band gaps of both α -Fe₂O₃ and α -Cr₂O₃. Optimised cell parameters were slightly greater than the experimental values, but the errors were less than 1.5% in both *a* and *c* and there was a clear decrease in both *a* and *c* from Fe₂O₃ to Cr₂O₃. Standard DFT B3LYP calculations gave slightly better optimised cell parameters but overestimated the direct band gaps. In both cases the calculated band gaps for the mixed oxide α -FeCrO₃ were close to that of α -Fe₂O₃. Inspection of the band structure showed that this was due to the lower edge of the conduction band being dominated by Fe3d in the two oxides. The upper edge of the valence band was dominated by Cr3d in the case of α -FeCrO₃, but this did not substantially alter the energy of the upper edge of the band. The band structure resembled that of Cr-doped α -Fe₂O₃. The lowest energy arrangement of Fe and Cr ions on the cation sites in α -FeCrO₃ is that with the ions ordered FeCrFeCr for the cations of the unit cell in ascending order

of z coordinate along the three-fold axis. This does not support the suggestion of an ordered centrosymmetric arrangement.

Our calculations show that there is little or no Fe-O-Cr π -type superexchange interaction and that the dominant coupling mechanism between Fe and Cr ions on sites 2 and 3 (and 1 and 4) is direct exchange giving ferromagnetic coupling. Hence for cells with the cations arranged FeCrFeCr or FeFeCrCr along the three-fold axis the lowest energy spin ordering was that characteristic of α -Fe₂O₃, $\uparrow\downarrow\downarrow\uparrow$. For FeCrCrFe we would expect cations on sites 1 and 2 and on sites 3 and 4 to be antiferromagnetically coupled, the Cr ions on sites 2 and 3 to be antiferromagnetically coupled and the Fe ions on sites 4 and 1 to be ferromagnetically coupled. It is impossible for all these couplings to be satisfied, thus this is a potentially spin-frustrated situation and may give rise to a spin glass. A sample of α -FeCrO₃ with each unit cell containing two Fe ions and two Cr ions but with the cation sites randomly occupied would be expected to show a net magnetic ordering similar to that of α -Fe₂O₃ as is observed experimentally.

Acknowledgements

The author would like to thank the following:

Anonymous referees for their helpful comments on the first draft of this paper which led me to consider the results of this work more deeply.

Prof. N. M. Harrison for providing his input file for α -Cr₂O₃.

The Open University Science Faculty for time on its Linux Beowulf cluster and G. Bradshaw for maintaining this system.

The EPSRC National Service for Computational Chemistry Software, URL:

<http://www.nscs.ac.uk> for time on the Columbus supercomputer facility.

Figure 1 was produced using Moldraw: P. Ugliengo, D. Viterbo, G. Chiari Z. Kristallogr. 207, 9 (1993) "MOLDRAW: Molecular Graphics on a Personal Computer.", P. Ugliengo "MOLDRAW: A Program to Display and Manipulate Molecular and Crystal Structures", Torino (2006) available on the web at: "<http://www.moldraw.unito.it>".

References

1. M. Catti and G. Sandrone, J. Chem. Soc. Faraday Discussions, **106**, 189 (1997).
2. B. N. Brockhouse, J. Chem. Phys., **21**, 961 (1953).
3. C. G. Shull, W. A. Strauser and E. O. Wollan, Phys. Rev., **83**, 333 (1951); T. G. Worton, R. M. Brugger and R.B. Bewman, J. Phys. Chem. Solids, **29**, 435 (1968).
4. T. Uozumi, K. Okada and A. Kotani, J. Electron Spectrosc. Relat. Phenom., **78**, 103 (1996); A. Fujimori, M. Saeki, N. Kimizuka, M. Taniguchi and S. Suga, Phys. Rev. B **34**, 7318 (1989); F. Ciccacci, L. Braicovich, E. Puppini and E. Vescovo, *ibid*, **44**, 10444 (1991).
5. T. Uozumi, K. Okada and A. Kotani, J. Electron Spectrosc. Relat. Phenom., **78**, 103 (1996); R. Zimmerman, P. Steiner and S. Hüfner, *ibid*, **78**, 49 (1996); T. Uozumi, K. Okada, A. Kotani, R. Zimmerman, P. Steiner, S. Hüfner, Y. Tezuka and S. Shin, *ibid*, **83**, 9 (1997); X. Li, L. Liu and V. E. Heinrich, Solid State Commun., **84**, 1103 (1992).
6. T. Uozumi, K. Okada, A. Kotani, R. Zimmerman, P. Steiner, S. Hüfner, Y. Tezuka and S. Shin, J. Electron Spectrosc. Relat. Phenom., **83**, 9 (1997).
7. T. Grygar, P. Bezdička and E. G. Caspary, J. Electrochem. Soc., **146**, 3234 (1999); H. E. V. Steinwehr, Z. Kristallogr., **125**, 377 (1967).

8. T. Grygar, P. Bezdička, J. Dědeček, E. Petrovsky and O. Schneeweis, *Ceramics*, **4**, 32 (2003).
9. K. F. McCarty, and D. R. Boehme, *J. Solid State Chem.*, **79**, 19 (1989); G. Busca, G. Ramis, M. del Carmen Prieto and V. S. Escibano, *J. Mater. Chem.*, **3**, 665 (1993); M. I. Baraton, G. Busca, M. C. Prieto, G. Ricchiardi and V. Sanchez Escibano, *J. Solid State Chem.*, **112**, 9 (1994).
10. M. Catti, G. Sandrone, G. Valerio and R. Dovesi, *J. Phys. Chem. Solids*, **57**, 1735 (1996); M. Catti, G. Valerio and R. Dovesi, *Phys. Rev. B*, **51** 7441 (1995).
11. L. M. Sandratskii, M. Uhl and J. Kübler, *J. Phys.; Condensed Matter*, **8**, 983 (1996).
12. M. P. J. Punkkinen, K. Kokko, W. Hergert and I. J. Väryynen, *J. Phys. Condensed Matter*, **11**, 2341 (1999).
13. A. Bandyopadhyay, J. Velez, W. H. Butler, S. [K](#), Sarker and O. Bengone, *Phys. Rev. B*, **69**, 174429 (2004).
14. A. Y. Dobin, W. Duan and R. M. Wentzcovitch, *Phys. Rev. B* **62**, 11997 (2000).
15. A. Rohrbach, J. Hafner and G. Kresse, *Phys. Rev. B* **70**, 125426 (2004).
16. J. Muscat, A. Wander and N. M. Harrison, *Chem. Phys. Lett.*, **342**, 397 (2001).
17. A. D. Becke, *J. Chem. Phys.*, **98**, 5648 (1993); S. H. Vosko, L. Wilk and M. Nusair, *Can. J. Phys.*, **58**, 1200 (1980).
18. C. Lee, W. Yang and R. G. Parr, *Phys. Rev. B*, **37**, 785 (1988).
19. J. Velez, A. Bandyopadhyay, W. H. Butler and S. J. Sarker, *Phys. Rev. B*, **71**, 205208 (2005).
20. V. R. Saunders, R. Dovesi, C. Roetti, R. Orlando, C. M. Zicovich-Wilson, N. M. Harrison, K. Doll, B. Civalleri, I. Bush, Ph. D'Arco, M. L. Lunell, *CRYSTAL2003 User's Manual*, University of Torino, Torino, 2003.

Deleted: J

Deleted:

21. R. Dovesi, V. R. Saunders, C. Roetti, R. Orlando, C. M. Zicovich-Wilson, F. Pascale, B. Civalleri, K. Doll, N. M. Harrison, I. J. Bush, Ph. D'Arco, M. LLunell, CRYSTAL06 User's Manual, University of Torino, Torino, 2006.
22. X. Feng and N. M. Harrison, *Phys. Rev. B*, **70**, 092402 (2004)
23. F. Cora, M. Alfredsson, G. Mallia, D. S. Middlemiss, W. C. Mackrodt, R. Dovesi and R. Orlando, *Structure and Bonding*, **113**, 171 (2004).

TABLE I. Calculated energies of the ferro- and antiferro-magnetic states of α -FeCrO₃ relative to that of the lowest energy antiferromagnetic state as 0. The ordering of spins and cations is given as 1 2 3 4 along the c axis. Cell constants and atomic positions relaxed.

Arrangement of cations	Energy/meV per formula unit			
	antiferromagnetic		ferromagnetic	
	($\uparrow\downarrow\uparrow\downarrow$)	($\uparrow\downarrow\downarrow\uparrow$)	(↑↑↓↓)	
CrFeFeCr				
B3LYP	110.00	-	118.48	258.23
B3LYP 10%	125.76	-	144.72	380.70
FeCrFeCr				
B3LYP	-	0	81.87	282.24
B3LYP 10%	-	0	99.47	406.19
FeFeCrCr				
B3LYP	157.69	79.02	-	311.98
B3LYP 10%	173.81	85.20	-	443.17

TABLE II. Lattice constants, axial ratio (c/a), magnetic moments and direct band gap (E_g) for antiferromagnetic corundum-related α -Fe₂O₃, α -FeCrO₃ and α -Cr₂O₃.

Method	a/pm	c/pm	c/a	$\mu/(\mu_B/\text{cation})$	E_g/eV
α-Fe₂O₃					
UHF ¹²	511.2	13.820	2.70	4.74	~11
B3LYP	505.7	1388.3	2.75	4.21	3.31
B3LYP 10%	505.5	1393.9	2.76	4.04	1.93
GGA + U ¹⁶	506.7	1388.2	2.74	4.11	2.0
exp.	503.5	1374.7	2.73	4.9 ^a	2
α-FeCrO₃					
FeCrFeCr					
B3LYP	504.6	1374.2	2.72	4.21, 2.88	3.26
B3LYP 10%	505.1	1377.9	2.73	4.06, 2.81	1.95
CrFeFeCr					
B3LYP	505.0	1380.5	2.73	4.25, 2.93	3.15
B3LYP 10%	505.5	1385.9	2.74	4.11, 2.86	1.63
FeFeCrCr					
B3LYP	504.7	1374.8	2.72	4.24, 2.86	3.29

B3LYP 10%	505.3	1378.1	2.73	4.09, 2.78	1.65
exp	501.0	1362.8	2.72		
α-Cr₂O₃					
UHF ¹²	504.8	1373.5	2.72	2.99	~15
B3LYP	500.6	1374.8	2.75	2.92	4.4
B3LYP 10%	501.2	1377.9	2.75	2.87	3.0
GGA + U ¹⁶	507.3	1383.9	2.73	3.01	2.6
exp.	495.9	1359.3	2.74	2.76 ^b	3.4

^a E. Kren, P. Szabo and G. Konczos, Phys. Lett., **19**, 103 (1965).

^b L.M. Corliss, J. M. Hastings, R. Nathans and G. Shirase, J. Appl. Phys., **36**, 1099 (1965).

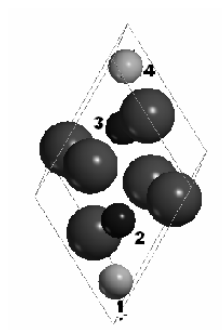
Figure captions

Figure 1 Primitive unit cell for corundum-type oxides α - M_2O_3 showing the labelling of the cation sites used in this paper; large spheres oxide ions, smaller spheres metal ions.

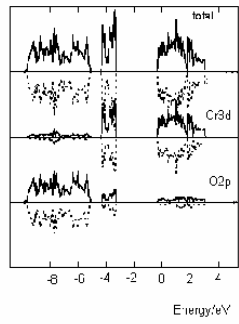
Figure 2. Total density of states and projection of M 3d and O 2p on the density of states for the most stable antiferromagnetic configurations of a) α - Fe_2O_3 and b) α - Cr_2O_3 from calculations using B3LYP with the Hartree-Fock exchange contribution reduced to 10%. Continuous line refers to 'spin-up' electrons and dotted line to 'spin-down' electrons.

Figure 3. Total density of states and projection of M 3d and O2p on the density of states for the most stable antiferromagnetic configurations of α - $FeCrO_3$ with a) cation ordering FeCrFeCr, b) cation ordering CrFeFeCr and c) cation ordering FeFeCrCr from calculations using B3LYP with the Hartree-Fock exchange contribution reduced to 10%. Continuous line refers to 'spin-up' electrons and dotted line to 'spin-down' electrons.

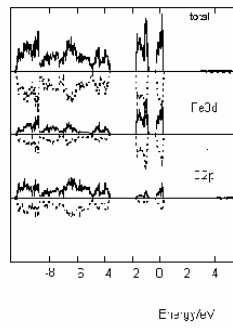
First Principles Study of Iron Chromium Oxide Figure 1



First Principles Study of Iron Chromium Oxide Figure 2

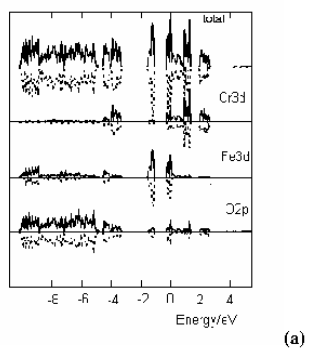


(a)

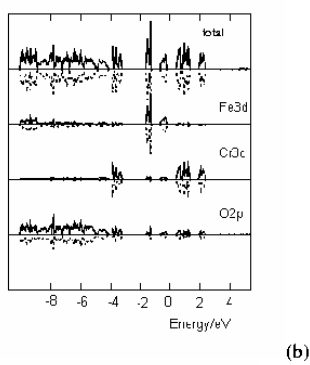


(b)

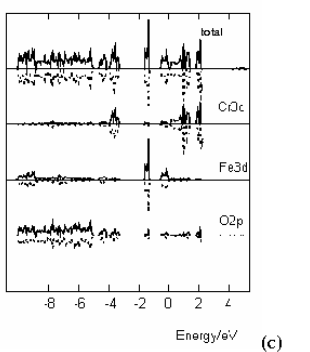
First Principles study of Iron Chromium Oxide Figure 3



(a)



(b)



(c)